Published in final edited form as:
J Neuropathol Exp Neurol. 2010 May ; 69(5): 473–482. doi:10.1097/NEN.0b013e3181dac07b.

Neuronal Damage in the Preterm Baboon: Impact of the Mode of Ventilatory Support

Catherine Verney, PharmD, PhD[1,2,3], **Sandra Rees, PhD, MSc, MPhil**[4], **Valérie Biran, MD, PhD**[1,2,3], **Merran Thompson, MBChB**[5], **Terrie Inder, MD, PhD**[6], and **Pierre Gressens, MD, PhD**[1,2,3,7]

[1]Inserm, U676, Paris, France

[2]Université Paris 7, Faculté de Médecine Denis Diderot, Paris, France

[3]PremUP, Paris, France

[4]Department of Anatomy and Cell Biology, University of Melbourne, Victoria, Australia

[5]Clinical Sciences Division, Imperial College, London, UK

[6]Department of Pediatrics, Neurology and Radiology, St. Louis Children's Hospital, Washington University, St. Louis, MO

[7]Institute for Reproductive and Developmental Biology, Imperial College, London, UK

Abstract

We evaluated the impact of randomized ventilatory strategies on specific neuronal populations of the cerebral cortex of preterm baboons. In the first series, baboons (n = 5) were delivered at 125 days of gestation (dg; term = 185 days) and exposed to 14 days of positive pressure ventilation (PPV) and compared to 140 dg controls (n = 6). In the second series, baboons were delivered at 125 dg and ventilated by either (i) PPV for 1 day followed by 27 days of nasal continuous positive airway pressure (early [EnCPAP]; n = 6) or (ii) PPV for 5 days followed by 23 days of CPAP (delayed [DnCPAP]; n = 4). Gestational controls were delivered at 153 dg (n = 3). The density of immunoreactive neurons for calretinin and somatostatin was assessed in the primary and secondary visual cortices, cingulate and parietal cortices and subiculum in paraffin sections. Compared to gestational controls, PPV for 14 days resulted in a reduction in the density of calretinin+ cells in the visual cortex (areas 17 and 18) but not in the other cortical areas. No effect of PPV was observed on somatostatin+ cells. DnCPAP, but not EnCPAP, was associated with a reduction in the density of calretinin and somatostatin+ cells in the visual cortical areas but not in the other cortical areas compared to gestational controls. Taken together, these data demonstrate that ventilatory strategies involving > 5 days of PPV have a regionally selective impact on cortical neuronal subpopulations within the visual area but not in areas of association cortex in a non-human primate model of prematurity.

Keywords

Cerebral palsy; Continuous positive airway pressure (CPAP); Cortex; Interneurons

Send correspondence and reprint requests to: Dr. Pierre Gressens, Inserm U 676, Hôpital Robert Debré, 48 Blvd. Sérurier, F-75019 Paris, France. Ph: +33 1 40 03 19 76; fax: +33 1 40 03 19 95; pierre.gressens@inserm.fr.

INTRODUCTION

Very preterm infants are at increased risk for the development of cerebral palsy, cognition, attention, executive function and perception deficits, and psychiatric symptoms (1,2). Some of these defects have been attributed to white matter damage (referred to as “periventricular leukomalacia”), including destruction and/or dysfunction of oligodendrocytes and axons (3-5). However, emerging evidence supports primary and secondary injury to grey matter (i.e. neuronal loss and/or neuronal abnormalities) associated with white matter injury that leads to the condition indicated by the broader term, “encephalopathy of prematurity”(6). For example, preterm infants with focal and diffuse white matter injury on magnetic resonance imaging tend to have reduced cerebral cortical and deep grey volumes (7,8). In addition, postmortem studies performed in preterm infants have shown neuronal abnormalities, including changes in neuronal nestin expression, increased neuronal inflammatory cytokine immunoreactivity, and aberrant neuronal circuitry and neuronal death (9-12).

It is plausible that these neuronal disturbances contribute to the functional deficits observed in preterm infants (13). Accordingly, investigation of the impact on perinatal and neonatal factors on grey matter is of importance. Epidemiological, clinical and experimental studies have identified several pre-, peri- and postnatal potential risk factors, particularly ventilatory strategies (14) that contribute to cerebral injury and/or adverse neurodevelopmental outcomes. Indeed, using the unique model of preterm delivery of baboon infants, Dieni et al showed that 14 days in neonatal intensive care unit conditions with positive pressure ventilation (PPV) delays brain growth when compared to control animals at the appropriate gestational age (15). Furthermore, Loeliger et al recently demonstrated that early nasal continuous positive airway pressure (EnCPAP) was associated with less white matter injury than delayed nasal continuous positive airway pressure (DnCPAP) therapy (16); both treatments were preceded by PPV.

Using the same non-human primate models of prematurity, we aimed to determine the impact of different ventilatory strategies on specific neuronal subpopulations in the cerebral cortex, with a special focus on gamma aminobutyric acidergic (GABAergic) interneurons (17,18). GABAergic interneurons represent about 20% of brain neurons (19,20) and are vulnerable after human perinatal brain injury (12). These GABAergic interneurons can be divided into different subpopulations based on the peptides and calcium-binding proteins (CaBPs) they express. In particular, interneurons expressing somatostatin (SST) are sensitive to hypoxic-ischemic injury in animal models (21,22). CaBPs are early markers of these interneuron subpopulations in developing primate cortices (17,18). Calretinin (CalR) is the earliest CaBP expressed in the non-human primate (23). Calbindin and parvalbumin are 2 other CaBPs that could be used to label subpopulations of interneurons in preterm baboons. However, calbindin expression seems to be transient in the developing cerebral cortex in primates (23) and parvalbumin, which is expressed in numerous cortical neurons in the adult brain, is a late marker during development and therefore could be absent in some cortical areas in preterm non-human primates (24).

The first goal of the present study was to determine whether PPV influences the subpopulations of CalR+ and SST+ GABAergic neurons as well as neuroglia (astrocytes and microglia) in the visual cortical areas and in other cortical areas (cingulate, parietal, subiculum) compared to age-matched gestational control animals. The second goal was to determine whether early extubation to nasal CPAP reduces the effects of PPV treatment of prematurity on these same neural subpopulations.

MATERIALS AND METHODS

All animal studies were performed at the Southwest Foundation for Biomedical Research in San Antonio, Texas. All animal husbandry, animal handling, and procedures were reviewed and approved to conform to American Association for Accreditation of Laboratory Animal Care guidelines. Timed gestations were determined by observing characteristic sex skin changes and confirmed by serial fetal ultrasound examinations.

Premature Baboons Treated with PPV Alone

Pregnant baboon dams (Papio papio) (n = 5) underwent elective hysterotomy and study animals were delivered at 125 ± 2 days of gestation (dg). This represents 67% of the term gestation of 185 days. At birth, the animals were weighed, sedated, intubated with a 2.0-mm endotracheal tube and treated with 4 mL/kg surfactant (Survanta, courtesy Ross Laboratories, Columbus, OH), prior to the initiation of PPV, on which they were maintained for 14 days. A complete description of the details of animal care including ventilator management, target goals for PaO_2, $PaCO_2$, tidal volume and nutritional, fluid and blood pressure management has been previously reported (25). Gestational control animals (n = 6) were delivered at 140 dg and killed immediately with sodium pentobarbitone. Neither group was treated with prenatal steroids.

Premature baboons treated with PPV and nasal CPAP

Pregnant baboon dams were treated with 6 mg of intramuscular betamethasone 48 and 24 hours prior to elective hysterotomy under general anesthesia. Study animals were delivered at 125 ± 2 dg, weighed, sedated, intubated with a 2.0-mm endotracheal tube and treated with 200 mg/kg Curosurf™ prior to the initiation of ventilator support. Gestational control animals (n = 3) were treated with betamethasone at 123 dg and 124 dg and delivered at 153 dg. The respiratory management of both EnCPAP (n = 6) and DnCPAP (n = 4) animals was initially identical and has been described previously in detail (26).

Extubation to nasal CPAP was attempted after either 24 hours (EnCPAP) or 5 days (DnCPAP) of PPV treatment. Animals were exposed for 27 days of CPAP in the EnCPAP group and for 23 days in the DnCPAP group. All animals were maintained on the Infant Flow Generator™ nasal CPAP delivery device (provided by EME -ElectroMedical Equipment- Ltd., Brighton, UK), via nasal prongs and occasionally nasal mask with an initial pressure of 7 cm H_2O. The animals were continued on nasal CPAP as long as there was an adequate respiratory drive. The criteria for this included a fraction of inspired oxygen (FiO_2) < 0.5, a pH >7.20, with no limit set for partial pressure of carbon dioxide ($PaCO_2$), provided the pH was maintained. If the nasal CPAP treatment failed, the animal was reintubated and ventilated with the least support to achieve adequate gas exchange and chest inflation. If the animal had minimal oxygen requirements (FiO_2 <0.25), good respiratory effort and no chest retractions, nasal CPAP was discontinued and the animal was placed in humidified supplementary oxygen or air. Nasal CPAP was reinstated if inspired FiO_2 exceeded 0.25 or poor respiratory effort or chest retractions were observed.

The management of nutrition, patent ductus arteriosus and hypotension have been previously described (27). Physiological variables including arterial blood gases (PaO_2, $PaCO_2$ and pH), arterial blood pressure, heart rate and FiO_2 were monitored continuously throughout the experimental period as previously reported (26,28).

Physiological Data

The “interval flux” of the physiological variables for the nasal CPAP cohort was calculated as a surrogate measure of the physiological instability of the animal (16). We first

determined the maximum and minimum values of each variable during a time interval (6 hourly time periods for the first 48 hours and daily periods thereafter). The "interval flux" was the difference between these values during the specified time period. For each animal, we identified the maximum flux and calculated the mean of the "interval fluxes" over the entire experimental period.

Neuropathological Scores

Neuropathological scores of damage/altered development were formulated from previously published quantitative data for the nasal CPAP cohorts (16). Scores for white matter (WM) included WM volume, ventricular volume, and density of astrocytes, and oligodendrocytes. For grey matter (GM), they included surface folding index (15), cortical volume and astrocyte density; for deep GM (i.e. basal ganglia and hippocampus) they included deep GM volume and hippocampal astrocyte density. The values for gestational controls were scored as 1 and mean values for each variable from the EnCPAP and DnCPAP animals were scored as; 1 if identical to controls; 2 (if up to ± 33% different from controls); 3 (from ± 33% to ± 66% different from controls); 4 (more than 66% different from controls). To estimate global brain alterations, scores for each variable were summed to give an overall score for WM, GM and deep GM for each animal.

Immunohistochemistry

Brains were removed, weighed, immersed in 4% paraformaldehyde in 0.1 M phosphate buffer, and processed to paraffin, as previously described (15). Eight-μm-thick coronal sections were selected in the rostro-caudal extension of the brain at the level of the hippocampal formation and more caudally at the level of the calcarine fissure. Sections were deparaffinized in a series of xylene/alcohol solutions. To enhance antibody penetration, sections were placed in citrate buffer 0.01 M for 2 cycles of 5 minutes each in a 600 W microwave oven. Sections were rinsed in 0.1 M phosphate buffer saline (PBS, pH 7.5) for 10 minutes and PBS-2% gelatin-0.5% Triton for 2 × 10 minutes. Primary antibodies were incubated for a week at 4°C in the above-described solution with 8% human serum albumin and 0.02% sodium azide. The primary reagents used were: rabbit polyclonal anti-CalR (1:2000; Swant, Bellinzona, Switzerland), goat polyclonal anti-SST (1:500; Santa Cruz Biotechnology, Santa Cruz, CA), mouse monoclonal anti-glial fibrillary acidic protein (GFAP) (1:500; Sigma, St. Louis, MO), and biotinylated *Ricinus* agglutinin 1 (RCA; 1:2000; Vector, Burlingame, CA). Labeling was visualized using the streptavidin-biotin-peroxidase complex (Amersham Biosciences, Orsay, France) (29) reacting with H_2O_2 (0.00 3%) as substrate in the presence of 3,3'-diaminobenzidine tetrahydrochloride (0.02%) as chromogen and with 0.6% nickel ammonium sulfate in 0.05 M TRIS buffer for enhancement. Counter-staining with neutral red was performed before dehydration and mounting in Pertex (Histolab, Göteborg, Sweden). To avoid regional and experimental variation in the intensity of labeling, sections from different experimental groups, including comparable anatomical regions, were stained together. Controls included omission of the primary antibody.

Quantification of Immunoreactive Cells

Counts of immunoreactive (IR) cells were performed in the cortical grey matter (layer II to VI) of visual areas 17 and 18 at the level of their boundary, the posterior cingulate area 23, the parietal cortex dorsal to the lateral fissure at the level of the operculum, and the subiculum of the hippocampal formation. These areas were selected to determine the impact of ventilatory strategies on different types of cortices, including primary visual cortex (area 17), secondary visual area (area 18) and other areas including the parietal cortex, posterior cingulate area and the subiculum. In the hippocampal formation, although CalR-IR somas and dendritic processes were previously observed in the presubiculum (30), the subiculum

was selected for quantitative analysis as the more dispersed CalR-IR cell bodies were more easily counted in this structure. Counts were made on coded slides blinded to the observer. For each animal and each cortical area studied, 2 or 3 non-adjacent sections were immunostained in successive experiments. Labeled cells from each section were counted in a 1 mm^2 (CalR and SST) or 0.25 mm^2 (GFAP and RCA) column encompassing the different layers of the cortical plate.

Statistical Analysis

Quantitative data are expressed as the mean ± SEM for each treatment group. Comparisons of results were conducted using Student *t* test or a one-way ANOVA with Dunnett's multiple comparison of means test. In EnCPAP and DnCPAP groups, correlations of immunohistochemical data with physiologic data, GFAP+ cell densities and neuropathological scores were performed by linear regression analyses. A $p < 0.05$ was considered significant.

RESULTS

Neocortical Distribution of Immunohistochemical Markers in Control Brains

In control brains at 140 dg and 153 dg, the CalR antibody preferentially stained cell bodies and proximal dendritic processes (Figs. 1A, C, 2A). As previously described in the developing and adult monkey cortices (31), CalR-IR neurons were distributed throughout the different areas and layers with variable densities. At the gestational ages studied, layers II-III of the visual (Fig, 1A, 2A), cingulate (Fig. 1C) and parietal areas (data not shown) displayed numerous bipolar and radially oriented CalR-IR perikarya in contrast to the sparse, dispersed positive cells detected in layers IV-V-VI. In layer I, CalR-labeled Cajal-Retzius cells were associated with a dense CalR-IR axonal field. In addition, in the visual areas, a CalR-IR axonal field was identified in layer IV for area 18 and in layer IVc in area 17 (Fig. 1A). In the visual cortex (areas 17 and 18), the density of CalR-IR cells was higher in controls at 140 dg than in 153 dg (Figs. 3A, 4A). A similar difference in density was detected in the parietal cortex (data not shown).

In control brains at both gestational ages, SST-IR cells (Fig. 2G. 153 dg) were significantly less numerous than CalR-IR cells in the different areas studied (Figs. 3A vs. 3B and 4A vs. 4B), which is in accord with studies in the developing and adult monkey brain (32,33). As in the developing macaque monkey cortex at similar ages (33), the distribution and density of SST+ cells varied in different cortical areas; however, at both ages the positive cells were located in layer V and VI (Fig. 2G). Interestingly, (as in the macaque cortex), baboon SST-IR cells had 2 main phenotypes, either small immunolabeled perikarya or a large perikaryon with bipolar or multipolar processes (Fig. 2G, H). Several large SST+ cells were dispersed in the subplate layer-intermediate zone and layer 1 displayed a dense network of SST+ axons (data not shown). There appeared to be no difference in SST-IR cell density between 140 and 153 dg in the areas studied (Figs. 3B, 4B).

A few GFAP+ cell bodies (Figs. 2D, 3C, 4C) displaying some processes and dispersed RCA + cells (Figs. 3D, 4D) were detected in the cerebral cortical layers of the control brains at both gestational ages.

Impact of PPV on Neocortical Immunohistochemical Markers

PPV for 14 days did not induce any detectable change in the global distribution of CalR, SST, GFAP or RCA compared to 140 dg controls (Fig. 1 and data not shown). The premature PPV group, however, had significantly reduced density of CalR-IR cells in areas 17 and 18 of the visual cortex compared to 140 dg controls (Figs. 1A vs. B and 3A). There

was no decrease detected in the parietal cortex, cingulate cortex or subiculum (Figs 1C vs. 1D and 3A). No effect in the PPV group was detectable in the density of SST-IR cells in any areas studied (Fig. 3B).

When compared to 140 dg controls, the PPV group had a significantly increased density of GFAP-IR cells in areas 17 and 18 of the visual cortex but not in the cingulate cortex (Fig. 3C). In PPV-exposed preterm animals, GFAP-IR cells displayed more numerous processes than 140 dg controls. Finally, the PPV group had a significantly increased density of RCA-IR cells in the cingulate cortex, but not in the visual cortex compared to 140 dg controls (Fig. 3D). In PPV-exposed animals, the RCA-IR cells tended to be amoeboid with fewer processes than in 153 dg controls.

Impact of Delayed vs. Early Nasal CPAP on Neocortical Immunohistochemical Markers

DnCPAP and EnCPAP did not induce any significant change in the global distribution of CalR (Fig. 2A-C), SST (not shown), GFAP (Fig. 2D-F) or RCA (Fig. 2G-I) immunostaining compared to 153 dg controls (Fig. 2). However, the DnCPAP group, but not the EnCPAP group had a significantly reduced density of CalR-IR and SST-IR cells in areas 17 and 18 compared to 153 dg controls; no effect was detected in the parietal cortex, cingulate cortex or subiculum (Figs. 2A-C, G-I, 4A, B).

When compared to 153 dg controls, the DnCPAP group but not the EnCPAP group had a significantly increased density of GFAP+ cells in areas 17 and 18 but not in the cingulate cortex (Figs. 2D-F, 4C). In the DnCPAP animals, GFAP+ cells had more numerous processes than in the 153 dg controls. Finally, the DnCPAP and EnCPAP groups had significantly increased densities of RCA-IR cells in the cingulate cortex, but not in the visual cortex compared to 153 dg controls (Fig. 4D). In DnCPAP animals, the RCA-IR cells tended to be amoeboid with fewer processes than in 140 dg controls.

Correlations of Calretinin+ Cell Density with Neuropathological Scores and Physiological Parameters

There were no significant correlations between the density of CalR-IR cells in area 17 of the visual cortex of brains from 153 dg controls, DnCPAP and EnCPAP animals found when they were plotted against white matter, grey matter or deep grey matter neuropathological scores, (data not shown). Similarly, when the densities of CalR-IR cells in area 17 of the visual cortex of brains from DnCPAP and EnCPAP animals were plotted against pH, PaO_2 or $PaCO_2$, no consistent correlations were found (not shown). In contrast, there were significant negative correlations between the density of CalR-IR cells and the median and average flux in FiO_2 (Fig. 5A) and the density of GFAP-IR cells in area 17 of the visual cortex (Fig. 5B).

DISCUSSION

The salient feature of the present study is our demonstration that PPV for 14 days significantly reduced the density of CalR+ interneurons in the visual cortex of preterm baboons compared to gestational controls. Similarly, the group treated with PPV for 5 days followed by DnCPAP for 23 days also had significantly reduced densities of CalR+ and SST + interneurons in the visual cortex. In contrast, the group treated with PPV for 1 day followed by EnCPAP for 27 days had no detectable difference in CalR+ interneuron density in the visual cortex from gestational controls. This protective effect of early CPAP is in accord with our previous studies of this model (16,34).

The mechanisms by which ventilatory strategies impact cortical interneuron populations in the preterm baboon are not entirely clear. The density of CalR+ interneurons in the visual

cortex in the preterm PPV group did not correlate with the neuropathological scores of grey or white matter injury, suggesting that the reduction in the density of interneurons was not related to or secondary to cerebral injury. Moreover, the reduction in the density of CalR+ interneurons was not associated with a detectable microglial reaction. In contrast, the presence of an increased density of GFAP+ cells in the visual cortex suggests that there was a pathological event in this cortical area that directly affected the survival and/or maturation of cortical interneurons. This event appears to have regional specificity since there was little impact on the parietal cortex, cingulate cortex or subiculum.

Most studies on cortical neuronal development have been done on the macaque. Although the pregnancy lasts 20 days longer in baboon than in the macaque, it is reasonable to assume that exposure to ventilator therapy from 125 days gestation in the baboon would be a time point after all of the cortical neurons had been generated and the vast majority had reached their final positions (35). This would be particularly valid in relation to the visual cortical areas that have been shown to have a more accelerated maturation (36). In this context, the reduced density of CalR+ interneurons in the primary and secondary visual cortex corresponds either to a reduced expression of this CaBP in interneurons which are impaired in their maturation or to a selective cell death of a subpopulation of interneurons. The significant loss of GABA neurons (GAD67+) and of CalR+ neurons detected in frontal cortical areas in preterm infants following white matter lesion (12) are in favor of the selective neuronal death hypothesis.

The lack of vulnerability of CalR+ interneurons in the cingulate cortex, parietal cortex and subiculum may be related to the fact that these cortical areas have reached a less mature stage of development than the primary cortical visual areas in the preterm baboon (37). Indeed, the stage of maturation appears to be a critical determinant for the vulnerability to perinatal insults of different cell types, including neurons (38) and oligodendrocytes (39). Although we did not analyze all cortical regions, the visual cortex appears to be selectively vulnerable to the impact of ventilatory strategies at this gestational age in this model.

SST+ interneurons were not affected in the preterm 14 days PPV group, which is consistent with resistance of SST neurons in animal models of cerebral palsy, including repeated asphyxia in fetal sheep (40) and neonatal hypoxia-ischemia in rat (41). SST+ interneuron densities were, however, significantly reduced in the visual cortex of preterm baboons exposed to PPV followed by DnCPAP but not in baboons exposed to PPV followed by EnCPAP. Together, these data suggest that SST+ interneurons become vulnerable when postnatal survival is extended from 14 days (i.e. PPV alone) to 28 days (5 days PPV + 23 days DnCPAP).

As in preterm infants, attempts were made to reduce hypoxic episodes in the baboons but there were nevertheless variations in the animals' respiratory stability due to their immaturity. The animals with lower fluxes in the fraction of inspired oxygen required to maintain appropriate blood gases had a higher density of CalR interneurons. Additional studies would be necessary to determine whether episodes of hypoxia are a risk factor for reductions in the density of cortical interneurons.

Although there was no functional evaluation of the visual cortex of these preterm baboons, some functional consequences of deficits in specific populations of interneurons would be expected. In children born very prematurely, different visual tests performed during development have revealed deficits involving the visual cortical dorsal stream (42). The deficit in subpopulations of GABAergic neurons could play a key role during the onset of cortical activity and functions (43). The present data support the emerging hypothesis injury to grey matter as well as white matter is present in preterm infants (6).

In summary, we clearly show that ventilatory regimens influence the development of cortical neurons (e.g. specific classes of GABA-expressing neurons in the visual cortex) in prematurely delivered baboons. Because GABA plays a crucial role in cortical activation, such effects may have a long term influence on sensory function (43).

Acknowledgments

The authors thank the Southwest National Primate Center BPD Resource Center personnel led by Dr. Jacqueline Coalson and including the animal husbandry group (Drs. D. Carey and M. Leland) and the neonatal intensive care unit technicians. We are most grateful to Dr. Michelle Loeliger for analysis of the physiological data and preparation of the neuropathological scores, and to Drs. Emily Camm and Penny Dalitz for preparation of the baboon tissue.

The work was supported by the National Institute of Health with the facility support (P51 RR13986) and preterm primate grants (HL52636 and HL074942), by the Inserm, Université Paris 7, Fondation PremUP, and Fondation Grace de Monaco.

References

1. Larroque B, Ancel PY, Marret S, et al. Neurodevelopmental disabilities and special care of 5-year-old children born before 33 weeks of gestation (the EPIPAGE study): A longitudinal cohort study. Lancet 2008;371:813–20. [PubMed: 18328928]
2. Wood NS, Marlow N, Costeloe K, et al. Neurologic and developmental disability after extremely preterm birth EPICure Study Group. N Engl J Med 2000;343:378–84. [PubMed: 10933736]
3. Dammann O, Hagberg H, Leviton A. Is periventricular leukomalacia an axonopathy as well as an oligopathy? Pediatr Res 2001;49:453–7. [PubMed: 11264425]
4. Melhem ER, Hoon AH Jr, Ferrucci JT Jr, et al. Periventricular leukomalacia: Relationship between lateral ventricular volume on brain MR images and severity of cognitive and motor impairment. Radiology 2000;214:199–204. [PubMed: 10644124]
5. Mikkola K, Ritari N, Tommiska V, et al. Neurodevelopmental outcome at 5 years of age of a national cohort of extremely low birth weight infants who were born in 1996-1997. Pediatrics 2005;116:1391–400. [PubMed: 16322163]
6. Volpe JJ. Encephalopathy of prematurity includes neuronal abnormalities. Pediatrics 2005;116:221–5. [PubMed: 15995055]
7. Inder TE, Warfield SK, Wang H, et al. Abnormal cerebral structure is present at term in premature infants. Pediatrics 2005;115:286–94. [PubMed: 15687434]
8. Srinivasan L, Dutta R, Counsell SJ, et al. Quantification of deep gray matter in preterm infants at term-equivalent age using manual volumetry of 3-tesla magnetic resonance images. Pediatrics 2007;119:759–65. [PubMed: 17403847]
9. Okoshi Y, Mizuguchi M, Itoh M, et al. Altered nestin expression in the cerebrum with periventricular leukomalacia. Pediatr Neurol 2007;36:170–4. [PubMed: 17352950]
10. Kadhim H, Tabarki B, De Prez C, et al. Cytokine immunoreactivity in cortical and subcortical neurons in periventricular leukomalacia: Are cytokines implicated in neuronal dysfunction in cerebral palsy? Acta Neuropathol 2003;105:209–16. [PubMed: 12557006]
11. Marin-Padilla M. Developmental neuropathology and impact of perinatal brain damage. III: gray matter lesions of the neocortex. J Neuropathol Exp Neurol 1999;58:407–29. [PubMed: 10331430]
12. Robinson S, Li Q, Dechant A, et al. Neonatal loss of gamma-aminobutyric acid pathway expression after human perinatal brain injury. J Neurosurg 2006;104:396–408. [PubMed: 16776375]
13. Leviton A, Gressens P. Neuronal damage accompanies perinatal white-matter damage. Trends Neurosci 2007;30:473–8. [PubMed: 17765331]
14. Horbar JD, Badger GJ, Carpenter JH, et al. Trends in mortality and morbidity for very low birth weight infants, 1991-1999. Pediatrics 2002;110:143–51. [PubMed: 12093960]
15. Dieni S, Inder T, Yoder B, et al. The pattern of cerebral injury in a primate model of preterm birth and neonatal intensive care. J Neuropathol Exp Neurol 2004;63:1297–309. [PubMed: 15624766]

16. Loeliger M, Inder T, Cain S, et al. Cerebral outcomes in a preterm baboon model of early versus delayed nasal continuous positive airway pressure. Pediatrics 2006;118:1640–53. [PubMed: 17015557]

17. Yan YH, Van Brederode JF, Hendrickson AE. Transient co-localization of calretinin, parvalbumin, and calbindin-D28K in developing visual cortex of monkey. J Neurocytol 1995;24:825–37. [PubMed: 8576712]

18. Verney C, Derer P. Cajal-Retzius neurons in human cerebral cortex at midgestation show immunoreactivity for neurofilament and calcium-binding proteins. J Comp Neurol 1995;359:144–53. [PubMed: 8557843]

19. Hendry SH, Schwark HD, Jones EG, et al. Numbers and proportions of GABA-immunoreactive neurons in different areas of monkey cerebral cortex. J Neurosci 1987;7:1503–19. [PubMed: 3033170]

20. Van Brederode JF, Mulligan KA, Hendrickson AE. Calcium-binding proteins as markers for subpopulations of GABAergic neurons in monkey striate cortex. J Comp Neurol 1990;298:1–22. [PubMed: 2170466]

21. Freund TF, Ylinen A, Miettinen R, et al. Pattern of neuronal death in the rat hippocampus after status epilepticus. Relationship to calcium binding protein content and ischemic vulnerability. Brain Res Bull 1992;28:27–38. [PubMed: 1347249]

22. Guan J, Waldvogel HJ, Faull RL, et al. The effects of the N-terminal tripeptide of insulin-like growth factor-1, glycine-proline-glutamate in different regions following hypoxic-ischemic brain injury in adult rats. Neuroscience 1999;89:649–59. [PubMed: 10199602]

23. Yan YH, van Brederode JF, Hendrickson AE. Developmental changes in calretinin expression in GABAergic and nonGABAergic neurons in monkey striate cortex. J Comp Neurol 1995;363:78–92. [PubMed: 8682939]

24. Berger B, Alvarez C, Goldman-Rakic PS. Neurochemical development of the hippocampal region in the fetal rhesus monkey. I. Early appearance of peptides, calcium-binding proteins, DARPP-32, and monoamine innervation in the entorhinal cortex during the first half of gestation (E47 to E90). Hippocampus 1993;3:279–305. [PubMed: 8353610]

25. McCurnin DC, Yoder BA, Coalson J, et al. Effect of ductus ligation on cardiopulmonary function in premature baboons. Am J Respir Crit Care Med 2005;172:1569–74. [PubMed: 16179644]

26. Thomson MA, Yoder BA, Winter VT, et al. Delayed extubation to nasal continuous positive airway pressure in the immature baboon model of bronchopulmonary dysplasia: lung clinical and pathological findings. Pediatrics 2006;118:2038–50. [PubMed: 17079577]

27. Thomson MA, Yoder BA, Winter VT, et al. Treatment of immature baboons for 28 days with early nasal continuous positive airway pressure. Am J Respir Crit Care Med 2004;169:1054–62. [PubMed: 14962819]

28. Loeliger M, Inder TE, Dalitz PA, et al. Developmental and neuropathological consequences of ductal ligation in the preterm baboon. Pediatr Res 2009;65:209–14. [PubMed: 19047953]

29. Verney C, Milosevic A, Alvarez C, et al. Immunocytochemical evidence of well-developed dopaminergic and noradrenergic innervations in the frontal cerebral cortex of human fetuses at midgestation. J Comp Neurol 1993;336:331–44. [PubMed: 7903321]

30. Berger B, Alvarez C. Neurochemical development of the hippocampal region in the fetal rhesus monkey, III: calbindin-D28K, calretinin and parvalbumin with special mention of Cajal-Retzius cells and the retrosplenial cortex. J Comp Neurol 1996;366:674–99. [PubMed: 8833116]

31. Meskenaite V. Calretinin-immunoreactive local circuit neurons in area 17 of the cynomolgus monkey, Macaca fascicularis. J Comp Neurol 1997;379:113–32. [PubMed: 9057116]

32. Huntley GW, Hendry SH, Killackey HP, et al. Temporal sequence of neurotransmitter expression by developing neurons of fetal monkey visual cortex. Brain Res 1988;471:69–96. [PubMed: 2464414]

33. Yamashita A, Hayashi M, Shimizu K, et al. Ontogeny of somatostatin in cerebral cortex of macaque monkey: An immunohistochemical study. Brain Res Dev Brain Res 1989;45:103–11.

34. Rees SM, Loeliger MM, Munro KM, et al. Cerebellar development in a baboon model of preterm delivery: Impact of specific ventilatory regimes. J Neuropathol Exp Neurol 2009;68:605–15. [PubMed: 19458549]

35. Rakic P. Neurons in rhesus monkey visual cortex: Systematic relation between time of origin and eventual disposition. Science 1974;183:425–7. [PubMed: 4203022]

36. Kroenke CD, Van Essen DC, Inder TE, et al. Microstructural changes of the baboon cerebral cortex during gestational development reflected in magnetic resonance imaging diffusion anisotropy. J Neurosci 2007;27:12506–15. [PubMed: 18003829]

37. Goldman-Rakic PS. Development of cortical circuitry and cognitive function. Child Dev 1987;58:601–22. [PubMed: 3608641]

38. Marret S, Gressens P, Gadisseux JF, et al. Prevention by magnesium of excitotoxic neuronal death in the developing brain: An animal model for clinical intervention studies. Dev Med Child Neurol 1995;37:473–84. [PubMed: 7789657]

39. Khwaja O, Volpe JJ. Pathogenesis of cerebral white matter injury of prematurity. Arch Dis Child Fetal Neonatal Ed 2008;93:F153–61. [PubMed: 18296574]

40. Mallard EC, Waldvogel HJ, Williams CE, et al. Repeated asphyxia causes loss of striatal projection neurons in the fetal sheep brain. Neuroscience 1995;65:827–36. [PubMed: 7609881]

41. Ferriero DM, Arcavi LJ, Sagar SM, et al. Selective sparing of NADPH-diaphorase neurons in neonatal hypoxia-ischemia. Ann Neurol 1988;24:670–6. [PubMed: 2904792]

42. Atkinson J, Braddick O. Visual and visuocognitive development in children born very prematurely. Prog Brain Res 2007;164:123–49. [PubMed: 17920429]

43. Ben-Ari Y, Khalilov I, Represa A, et al. Interneurons set the tune of developing networks. Trends Neurosci 2004;27:422–7. [PubMed: 15219742]

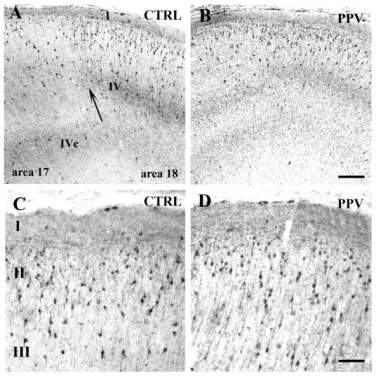

Figure 1.

Calretinin (CalR) immunoreactivity in the cortex of control (CTRL) (**A, C**) and positive pressure ventilation (PPV)-treated (**B, D**) preterm baboons at 140 days gestation. (**A, B**) Rostral visual cortex at the transitional level (arrow) between area 17 and area 18. In **A**, note the high density of mostly radially oriented bipolar CalR+ neurons in layers II-III and the dense positive fiber fields in layer IV (area 18) and layer IVc (area17). The CalR+ cells are less dense in **B**. (**C, D**) Superficial layers (I-II-III) of the cingulate cortex: no difference in density is detected between CRTL (**C**) and PPV-treated (**D**) animals. Scale bars: A, B: 200 μm, C, D: 60 μm.

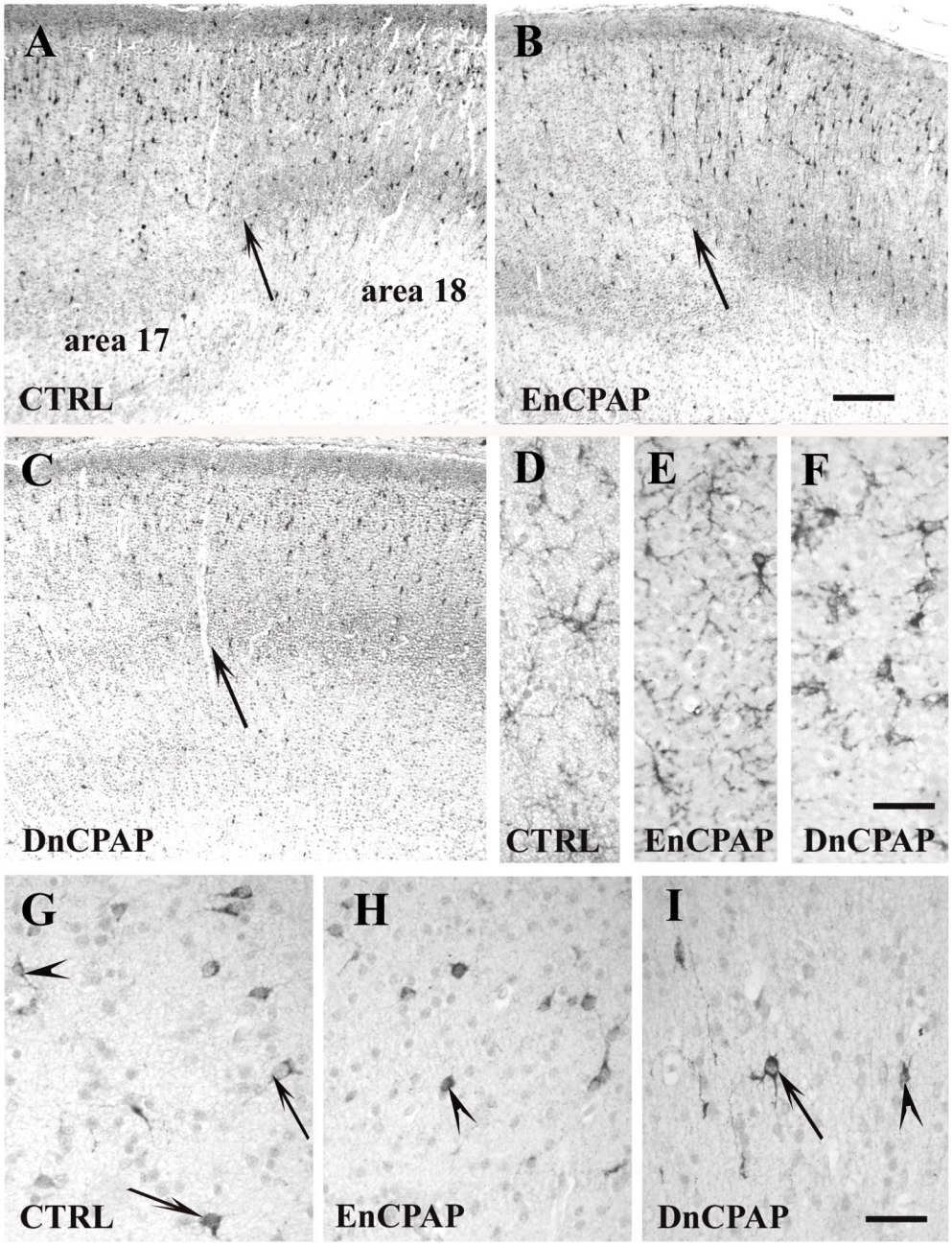

Figure 2.

Labeling of the visual cortex in control (CTRL) (**A, D, G**), early nasal continuous positive airway pressure (EnCPAP)-treated (**B, E, H**) and delayed CPAP (DnCPAP)-treated (**C, F, I**) preterm baboons at 153 days gestation. (**A–C**) Calretinin (CalR) immunoreactivity at the transition between area 17 and area 18 (arrow). (**D–F**) Glial fibrillary acidic protein (GFAP) + astrocytes in layer IV of the primary visual cortex (area 17). (**G–I**) Somatostatin (SST)+ neurons in layer V-VI in visual area 17. Note the large positive cell body (arrow) compared to smaller immunoreactive perikaryon (arrowheads). Scale bars: **A–C**: 200 μm, **D–I**: 30 μm.

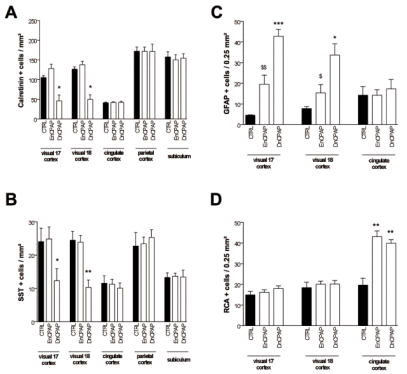

Figure 3.

Quantitative determination of the density of calretinin (CalR)+ (**A**), somatostatin (SST)+ (**B**), glial fibrillary acidic protein (GFAP)+ (**C**), and *Ricinus* agglutinin 1 (RCA)+ (**D**) cells in different regions of control and positive pressure ventilation (PPV)-treated preterm baboon infant at 140 days gestation. Bar represents mean density of positive cells ± SEM. Asterisks indicate statistically significant differences from black bars; **p < 0.01 in ANOVA with Bonferroni multiple comparison test.

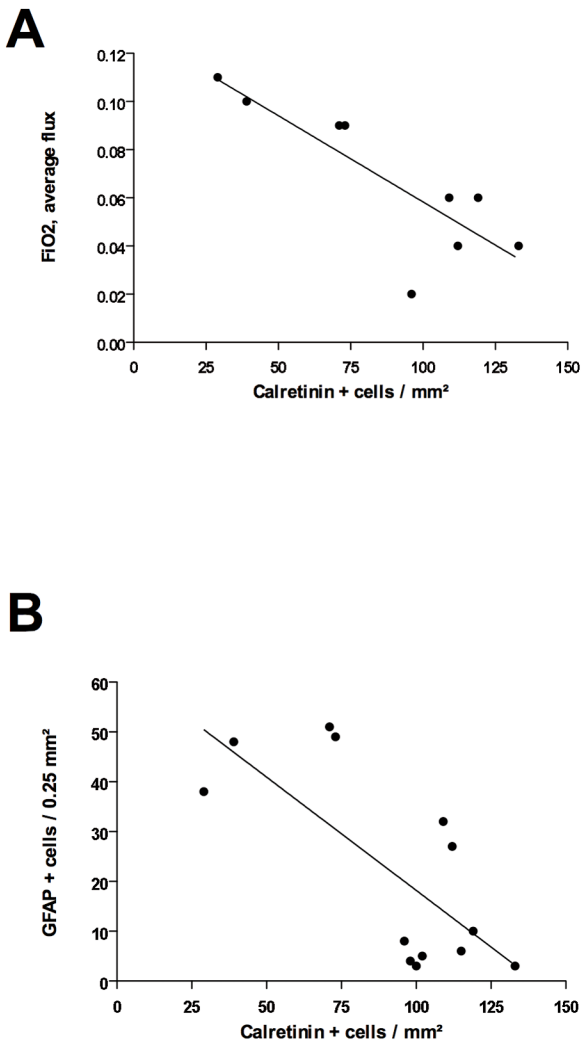

Figure 4.

Quantitative determination of the density of calretinin (CalR)+ (**A**), somatostatin (SST)+ (**B**), glial fibrillary acidic protein (GFAP)+ (**C**), and *Ricinus* agglutinin 1 (RCA)+ (**D**) cells in different regions of control, early nasal continuous positive airway pressure (EnCPAP), and delayed CPAP (DnCPAP) treated preterm baboon infant at 153 days gestation. Bars represent mean density of positive cells ± SEM. Asterisks indicate statistically significant differences from control group; "$" indicates statistically significant difference from DnCPAP group; *, $p < 0.05, $$p < 0.01, ***p < 0.001 in ANOVA with Bonferroni multiple comparison test.

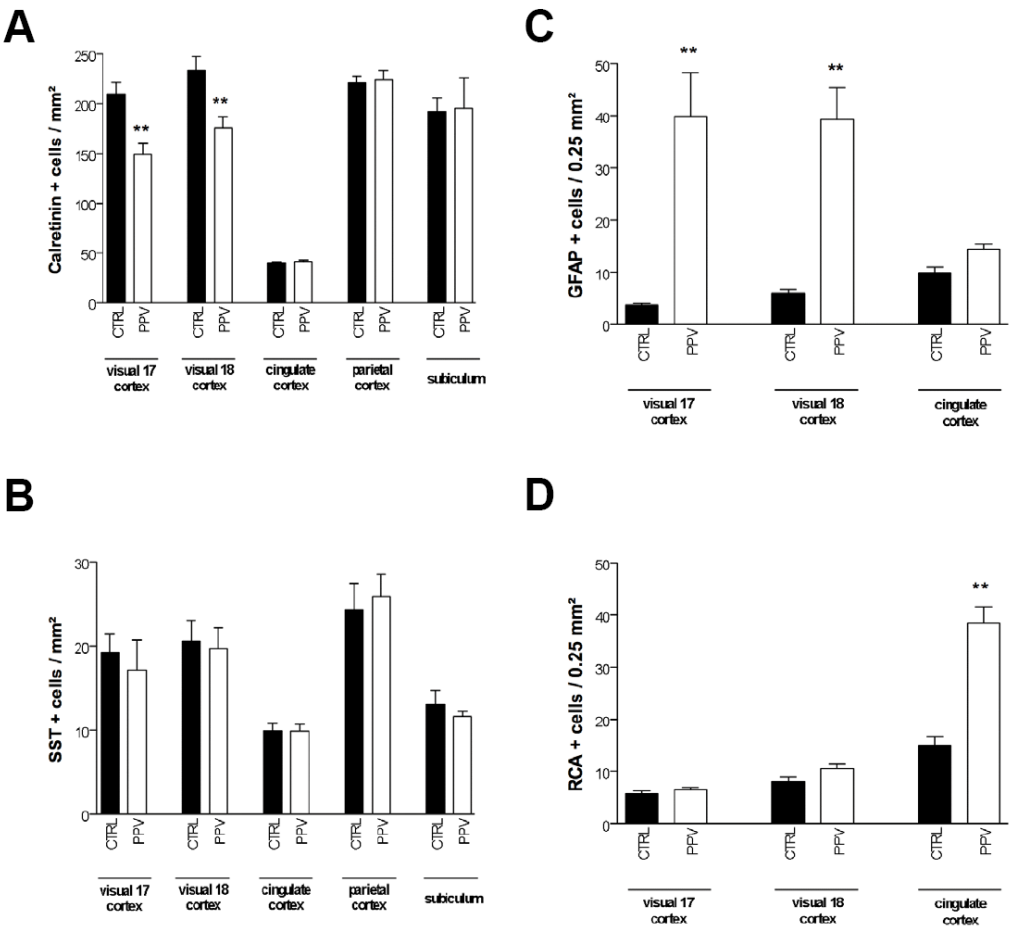

Figure 5.

Regression analyses between density of Calretinin (CalR)+ neurons in area 17 of the visual cortex and i) average flux in fraction of inspired oxygen (FiO_2)(**A**; $r^2 = 0.69$; $p < 0.01$) and ii) density of glial fibrillary acidic protein (GFAP)+ cells in area 17 of the visual cortex (**B**; $r^2 = 0.52$; $p < 0.01$).